

Neural Stochastic Partial Differential Equations

Cristopher Salvi¹ Maud Lemerrier² Andris Gerasimovičs³

Abstract

Stochastic partial differential equations (SPDEs) are the mathematical tool of choice to model dynamical systems evolving under the influence of randomness. By formulating the search for a mild solution of an SPDE as a neural fixed-point problem, we introduce the *Neural SPDE* model to learn solution operators of PDEs with (possibly stochastic) forcing from partially observed data. Our model provides an extension to two classes of physics-inspired neural architectures. On the one hand, it extends Neural CDEs, SDEs, RDEs – continuous-time analogues of RNNs – in that it is capable of processing incoming sequential information even when the latter evolves in an infinite dimensional state space. On the other hand, it extends Neural Operators – generalizations of neural networks to model mappings between spaces of functions – in that it can be used to learn solution operators $(u_0, \xi) \mapsto u$ of SPDEs (a.k.a. Itô maps) depending simultaneously on the initial condition u_0 and a realization of the driving noise ξ . A Neural SPDE is resolution-invariant, it may be trained using a memory-efficient implicit-differentiation-based backpropagation and, once trained, its evaluation is up to 3 orders of magnitude faster than traditional solvers. Experiments on various semilinear SPDEs, including the 2D stochastic Navier-Stokes equations, demonstrate how Neural SPDEs capable of learning complex spatiotemporal dynamics with better accuracy and using only a modest amount of training data compared to all alternative models.

(Li et al., 2020a), and rough (Morrill et al., 2021) differential equations (Neural CDEs, SDEs, RDEs). These models can be seen as continuous analogues of RNNs and are emerging as leading machine learning tools for modelling temporal dynamics in finite dimensional state spaces.

Many dynamical systems though, evolve in an infinite dimensional state space of functions and can best be described using the language of partial differential equations (PDEs). Neural Operators (Kovachki et al., 2021; Li et al., 2020c;b;d) are generalizations of neural networks offering an elegant way to learn mappings between spaces of functions, which makes them an attractive option for modelling PDE-dynamics. However, deterministic PDEs fail to incorporate randomness into the system they describe. In many cases the presence of noise leads to new phenomena, both at the mathematical and the physical level, generally describing more complex and realistic dynamics than the ones arising from deterministic PDEs.

Stochastic partial differential equations (SPDEs) are the mathematical tool of choice to model many physical, biological and economic systems subject to the influence of randomness, be it intrinsic (e.g. quantifying uncertainty) or extrinsic (e.g. modelling environmental random perturbations). Examples include the *Kardar–Parisi–Zhang (KPZ) equations* for random interface growth modelling for instance the propagation of a forest fire from a burnt region to an unburnt region (Hairer, 2013), the Φ^4 -models describing phase transitions of ferromagnets and superconductors near critical temperatures (Kleinert & Schulte-Frohlinde, 2001), or the *stochastic Navier-Stokes equations* modelling the dynamics of a turbulent fluid flow under the presence of local random fluctuations (Mikulevicius & Rozovskii, 2004). For an introduction to SPDEs see (Hairer, 2009); a comprehensive textbook is (Holden et al., 1996).

While Neural Operators can be used to learn operators mapping the initial condition u_0 or a realization of the forcing noise ξ to the solution u of a PDE, they are not designed to handle SPDEs where solutions depend simultaneously on u_0 and ξ . Using the notion of mild solution to an SPDE and some basic semigroup theory, we resolve this issue and introduce the *neural stochastic partial differential equation* (Neural SPDE) model to learn solution operators of the form $(u_0, \xi) \mapsto u$ from partially observed data.

1. Introduction

Interest in combining differential equations and deep learning has recently given rise to a large variety of neural differential equation architectures for modelling temporal dynamics such as neural controlled (Kidger et al., 2020), stochastic

¹Imperial College London & The Alan Turing Institute, UK
²University of Warwick, UK ³University of Bath, UK. Correspondence to: Cristopher Salvi <csalvi@ic.ac.uk>.

We perform experiments on various semilinear SPDEs, including the stochastic Navier-Stokes equations in 2 spatial dimensions. The outcomes illustrate several aspects of our model: 1) it is resolution-invariant, which means that even if trained on a lower resolution it can be directly evaluated on a higher resolution without sacrificing performance; 2) it requires a lower amount of training data compared to alternative neural-differential-equations-based and Neural-Operators-based models; 3) it is up to 3 orders of magnitude faster than traditional SPDE solvers.

The outline of the paper is as follows: in Sec. 2 we present related work on neural differential equations and Neural Operators, in Sec. 3 we provide a brief introduction to the theory of SPDEs which will help us defining our Neural SPDE model in Sec. 4. In Sec. 5 we present experiments on various semilinear SPDEs, including the stochastic Navier-Stokes equations.

2. Related work

In this section we provide a brief introduction to some popular neural differential equation models for temporal dynamics in finite dimensional state spaces as well as to Neural Operators, a recent generalization of neural network to infinite dimensional spaces of functions.

Let $T > 0$ and $d, d_u, d_\xi, d_h \in \mathbb{N}$.

2.1. Neural ODEs

A neural ordinary differential equation (Neural ODE), as popularised by (Chen et al., 2018), is a parametric model with initial input $u_0 \in \mathbb{R}^{d_u}$ consisting of: a feedforward neural network $\ell_\theta : \mathbb{R}^{d_u} \rightarrow \mathbb{R}^{d_h}$ lifting the solution to a hidden space \mathbb{R}^{d_h} , where d_h is a hyperparameter chosen by the user, a feedforward neural network $f_\theta : \mathbb{R}^{d_h} \rightarrow \mathbb{R}^{d_h}$ (with some minimum Lipschitz regularity) modelling the vector field of an ODE in hidden space, and a linear projection $\pi_\theta : \mathbb{R}^{d_h} \rightarrow \mathbb{R}^{d_u}$. The forward pass can be written as

$$z_0 = \ell_\theta(u_0), \quad z_t = z_0 + \int_0^t f_\theta(z_s) ds, \quad u_t = \pi_\theta(z_t). \quad (1)$$

The integral in (1) can be evaluated numerically via a call to an ODE solver of choice (Euler, Runge-Kutta, adaptive schemes...). The output u_t is then fed to a loss function (mean squared, cross entropy etc.) and trained via stochastic gradient descent in the usual way.

As described in (Chen et al., 2018), backpropagation can be done efficiently via the adjoint sensitivity method (Pontryagin, 1987) by solving additional ODEs for the gradients of the loss instead of backpropagating through the operations of the ODE solver.

However, the output of a Neural ODE is determined only by the initial condition u_0 , and there is no direct mechanism

for adjusting the trajectory based on data that arrives at later times (Ciccone et al., 2018).

2.2. Neural CDEs, SDEs, RDEs

Controlled differential equations (CDEs) (Lyons, 1998; 2014; Lyons et al., 2007) allow to resolve this issue by incorporating incoming information into the dynamics of an ODE. Given an initial condition $u_0 \in \mathbb{R}^{d_u}$ and some time-dependent information (usually a time series) interpolated into a continuous path $\xi : [0, T] \rightarrow \mathbb{R}^{d_\xi}$ of bounded variation, a Neural CDE (Kidger et al., 2020) uses the same neural networks $\ell_\theta, f_\theta, \pi_\theta$ as in a Neural ODE as well as an additional matrix-valued neural network $g_\theta : \mathbb{R}^{d_h} \rightarrow \mathbb{R}^{d_h \times d_\xi}$ (satisfying some minimal Lipschitz regularity)¹. Then, the forward pass of a Neural CDE is written as follows

$$\begin{aligned} z_0 &= \ell_\theta(u_0), \\ z_t &= z_0 + \int_0^t f_\theta(z_s) ds + \int_0^t g_\theta(z_s) d\xi_s, \\ u_t &= \pi_\theta(z_t), \end{aligned} \quad (2)$$

where the second integral is interpreted in the Riemann–Stieltjes sense. In (Kidger et al., 2020), the control ξ is obtained using cubic splines interpolation on the original data so that the term " $d\xi_s$ " can be interpreted as " $\dot{\xi}_s ds$ ". Therefore, eq. (2) becomes an ODE; forward and backward passes can be carried out as they would in a Neural ODE.

Neural stochastic differential equations (Neural SDEs) are special classes of Neural CDEs where the control ξ is a sample path from a \mathbb{R}^{d_ξ} -dimensional Brownian motion and where the integral is a stochastic integral understood in the Stratonovich sense $\int_0^t g_\theta(z_s) \circ d\xi_s$. Neural SDEs can be used as generative models (trained either as VAEs or GANs) for path-valued random variables (Kidger et al., 2021).

Neural rough differential equations (Neural RDEs) (Morrill et al., 2021) extend Neural CDEs in that they allow to relax the regularity assumption on ξ and consider a larger class of controls and are particularly well suited for long time series. However, they rely on a path transform, the *log-signature*, that increases exponentially the dimensionality of the input stream ξ , making Neural RDEs impractical for high dimensional time series ($d_\xi \gg 1$).

As for Neural ODEs, a similar memory-efficient approach can be used to train a Neural CDE (SDE, RDE resp.) avoiding backpropagating the errors through the operations of the numerical solver. In effect, it is shown in (Kidger et al., 2020; Morrill et al., 2021) that the gradients of the loss with

¹In (Kidger et al., 2020) the control path ξ is "augmented-with-time" to form a new path $\hat{\xi}_t = (t, \xi_t) \in \mathbb{R}^{d_\xi+1}$ so that the update in eq. (2) can be rewritten more compactly as $z_t = z_0 + \int_0^t h_\theta(z_s) d\hat{\xi}_s$, where $h_\theta : \mathbb{R}^{d_h} \rightarrow \mathbb{R}^{d_h \times (d_\xi+1)}$ is another neural network.

respect to the model parameters are solutions of linear CDEs (SDEs, RDEs reps.) and so can be obtained by another call to the numerical solver.

Neural CDEs, SDEs, RDEs are continuous-time sequential models that can be used to learn differential equations where $u_0 \in \mathbb{R}^{d_u}$ is a vector, and where the solution $u : [0, T] \rightarrow \mathbb{R}^{d_u}$ and control $\xi : [0, T] \rightarrow \mathbb{R}^{d_\xi}$ are continuous paths with values in finite dimensional state spaces $\mathbb{R}^{d_u}, \mathbb{R}^{d_\xi}$ respectively. Despite being time-resolution invariant, these neural differential equation models are not space-resolution invariant. Hence, they cannot be deployed to learn dynamics in infinite dimensional state spaces, such as the ones described by partial differential equations (PDEs), due to the non-linear interactions between the various space-time points typically observed in PDE-dynamics.

2.3. Neural Operators

Neural Operators (Kovachki et al., 2021; Li et al., 2020c;b) are generalizations of neural networks offering an efficient way to model mappings between spaces of functions. Contrary to the previous differential equation models, Neural Operators can be used to model mappings of the form $u_0 \mapsto u$, where $u_0 : \mathcal{D} \rightarrow \mathbb{R}^{d_u}$ is the initial condition and $u : \mathcal{D} \rightarrow \mathbb{R}^{d_u}$ is the solution of an underlying PDE, and where $\mathcal{D} \subset \mathbb{R}^d$ is a bounded domain.

Contrary to prior work attempting to merge PDEs and deep learning techniques, Neural Operators do not require knowledge of the exact form of the underlying PDE, they are resolution-invariant and they achieve superior performance compared to previous deep-learning-based PDE solvers.

Given an initial condition $u_0 : \mathcal{D} \rightarrow \mathbb{R}^{d_u}$, a Neural Operator with M layers is defined as an architecture of the form

$$\begin{aligned} z^0(x) &= L_\theta(u_0(x)), \\ z^k(x) &= N_\theta^k(z^{k-1})(x), \\ u^{\text{out}}(x) &= \Pi_\theta(z^M(x)), \end{aligned} \quad (3)$$

for $x \in \mathcal{D}$ and $k = 1, \dots, M$, where $L_\theta : \mathbb{R}^{d_u} \rightarrow \mathbb{R}^{d_h}$ and $\Pi_\theta : \mathbb{R}^{d_h} \rightarrow \mathbb{R}^{d_u}$ are feedforward neural networks and each N_θ^k is a parametric operator defined for any $z : \mathcal{D} \rightarrow \mathbb{R}^{d_h}$ as

$$N_\theta^k(z)(x) := \sigma\left(A_\theta^k z(x) + b_\theta^k + \int_{\mathcal{D}} \mathcal{K}_\theta^k(x, y) z(y) dy\right) \quad (4)$$

where $A_\theta^k \in \mathbb{R}^{d_h \times d_h}$, $b_\theta^k \in \mathbb{R}^{d_h}$, $\mathcal{K}_\theta^k : \mathcal{D}^2 \rightarrow \mathbb{R}^{d_h \times d_h}$ is a matrix-valued kernel and σ is an activation function.

Remark 1 *In the case of evolution-type PDEs, the solution $u : [0, T] \times \mathcal{D} \rightarrow \mathbb{R}^{d_u}$ also depends on time. There are two ways of dealing with such time-dependent problems using Neural Operators. One can either consider $\tilde{\mathcal{D}} = [0, T] \times \mathcal{D}$ as the new input domain, or use an auto-regressive structure*

in time to model the mapping $z(t_{i-1}, \cdot) \rightarrow z(t_i, \cdot)$ as per (4). This allows to use Neural Operators for learning mappings of the form $\xi \mapsto u$, where $\xi : [0, T] \times \mathcal{D} \rightarrow \mathbb{R}^{d_\xi}$ is a (possibly stochastic) time-dependent forcing term of the PDE.

2.4. Fourier Neural Operators

Among all kinds of Neural Operators, Fourier Neural Operators (FNOs) (Li et al., 2020d) stand out because of their easier parametrization while maintaining similar learning performance. In a FNO, each kernel \mathcal{K}_θ^k is assumed to be stationary so that $\mathcal{K}_\theta^k(x, y) = \mathcal{K}_\theta^k(x - y)$. With this assumption, the integral in eq. (4) becomes a convolution (\ast_d):

$$N_\theta^k(z)(x) = \sigma\left(A_\theta^k z(x) + b_\theta^k + (\mathcal{K}_\theta^k \ast_d z)(x)\right) \quad (5)$$

The main remark made in Li et al. (2020d) is to use the convolution theorem and rewrite eq. (5) in terms of the d -dimensional Fourier Transform \mathcal{F}_d and its inverse \mathcal{F}_d^{-1}

$$\begin{aligned} N_\theta^k(z)(x) &= \sigma\left(A_\theta^k z(x) + b_\theta^k \right. \\ &\quad \left. + \mathcal{F}_d^{-1}\left(\mathcal{F}_d(\mathcal{K}_\theta^k) \mathcal{F}_d(z)\right)(x)\right). \end{aligned} \quad (6)$$

As argued in Li et al. (2020d), assuming that the kernel \mathcal{K}_θ^k is periodic on \mathcal{D} , instead of working with the Fourier Transform $\mathcal{F}_d(\mathcal{K}_\theta^k)$, one can consider its Fourier series expansion and truncate it at a maximal number of frequency modes $\omega_1^{\max}, \omega_2^{\max}, \dots, \omega_d^{\max} \in \mathbb{N}$. This allows to parameterize $\mathcal{F}_d(\mathcal{K}_\theta^k)(\omega)$, for any frequency mode $\omega \in \mathcal{D}$, directly in Fourier space as a complex $(2\omega_1^{\max} \times \dots \times 2\omega_d^{\max} \times d_h \times d_h)$ -tensor K_θ^k and rewrite eq. (6) as follows

$$\begin{aligned} N_\theta^k(z)(x) &= \sigma\left(A_\theta^k z(x) + b_\theta^k \right. \\ &\quad \left. + \mathcal{F}_d^{-1}\left(K_\theta^k \mathcal{F}_d(z)\right)(x)\right), \end{aligned} \quad (7)$$

where the multiplication $K_\theta^k \mathcal{F}_d(z)$ is a matrix-vector multiplication². Assuming uniform sampling of observations across space, the Fourier Transform can be approximated by the Fast Fourier Transform (Li et al., 2020d, Section 4).

Despite the ability of FNOs to learn operators mapping either the initial condition u_0 or a time-dependent forcing ξ to the solution u of a PDE, these models offer no natural mechanism to learn solution operators mapping the pair (u_0, ξ) to the solution u (a.k.a. Itô map), which is crucial for solving SPDEs. Furthermore, as highlighted in the conclusion of Li et al. (2020d), in order to learn complex PDEs, FNOs require a large amount of training samples, which is a hard constraint to satisfy, as data generation is generally a very

²For any frequency mode $\omega \in \mathcal{D}$ one has $\mathcal{F}_d(z)(\omega) \in \mathbb{C}^{d_h}$ and $\mathcal{F}_d(K_\theta^k)(\omega) \in \mathbb{C}^{d_h \times d_h}$.

expensive procedure. In addition, the number of learnable parameters in an FNO is usually very high, mainly because the weights are not shared among the different layers, making the model memory-consuming.

We note that an interesting line of work to tackle SPDE-learning is provided in the recent paper Chevyrev et al. (2021). The authors construct a set of features from the pair (u_0, ξ) following the definition of a *model* from the theory of *regularity structures* (Hairer, 2014). Then, they perform linear regression from this set of features to the solution of the SPDE at a specific space-time point $(t, x) \in [0, T] \times \mathcal{D}$. However, contrary to all other benchmarks considered in this paper, one would have to fit a different regression function for each space-time point. In addition, this model assumes knowledge of the leading differential operator in the SPDE. For these reasons we do not include this recent line of work as one of our benchmarks.

In the next section we provide some theoretical background on SPDEs.

3. Background on SPDEs

For simplicity, we will assume that all functions discussed in this section are complex valued. Let $\mathcal{D} \subset \mathbb{R}^d$ be a bounded domain. Let $\mathcal{H}_u = \{f : \mathcal{D} \rightarrow \mathbb{C}^{d_u}\}$ and $\mathcal{H}_\xi = \{f : \mathcal{D} \rightarrow \mathbb{C}^{d_\xi}\}$ be two Hilbert spaces of functions on \mathcal{D} with values in \mathbb{C}^{d_u} and \mathbb{C}^{d_ξ} respectively.

We consider a large class of SPDEs of parabolic type

$$du_t = (\mathcal{L}u_t + F(u_t))dt + G(u_t)d\xi_t \quad (8)$$

where ξ_t is an infinite dimensional Q -Wiener process (Lord et al., 2014, Definition 10.6) or a cylindrical Wiener process (Hairer, 2009, Definition 3.54), $F : \mathcal{H}_u \rightarrow \mathcal{H}_u$ and $G : \mathcal{H}_u \rightarrow L(\mathcal{H}_\xi, \mathcal{H}_u)$ are two continuous functions, with $L(\mathcal{H}_\xi, \mathcal{H}_u)$ denoting the space of bounded linear operators from \mathcal{H}_ξ to \mathcal{H}_u , and where \mathcal{L} is a linear differential operator generating a *semigroup* $S_t : \mathcal{H}_u \rightarrow \mathcal{H}_u$. For a primer on semigroup theory see Hairer (2009, Section 4).

A function $u : [0, T] \rightarrow \mathcal{H}_u$ is a *mild solution* to the SPDE (8) if for any $t \in [0, T]$ it satisfies

$$u_t = S_t u_0 + \int_0^t S_{t-s} F(u_s) ds + \int_0^t S_{t-s} G(u_s) d\xi_s, \quad (9)$$

where the second integral is a stochastic integral (Hairer, 2009, Definition 3.57). An SPDE can be informally thought of as an SDE with solutions evolving in an infinite dimensional state space \mathcal{H}_u and driven by an infinite dimensional "Brownian motion" ξ .

3.1. A fixed point problem

Assuming global Lipschitz regularity on the functions F and G , a solution $u : [0, T] \rightarrow \mathcal{H}_u$ to Equation (8) exists and is unique (Hairer, 2009, Theorem 6.4).

The proof relies on the Banach fixed point theorem (also known as the contraction mapping theorem) and works in almost exactly the same way as the usual proof of uniqueness of solution for ODEs with Lipschitz vector fields. The main argument, which will be central for the construction of our model in the next section, asserts that under these conditions, the operator $\Phi^\xi : C([0, T], \mathcal{H}_u) \rightarrow C([0, T], \mathcal{H}_u)$ depending on ξ and defined for any $t \in [0, T]$ as

$$\begin{aligned} \Phi^\xi(u)_t &= S_t u_0 + \int_0^t S_{t-s} F(u_s) ds + \int_0^t S_{t-s} G(u_s) \dot{\xi}_s ds \\ &= S_t u_0 + \int_0^t S_{t-s} H^{u, \xi}(s, \cdot) ds, \end{aligned} \quad (10)$$

is a contraction, and where $H^{u, \xi} : [0, T] \times \mathcal{D} \rightarrow \mathbb{C}^{d_u}$ is defined as follows

$$H^{u, \xi}(t, x) := (F(u_t) + G(u_t) \dot{\xi}_t)(x). \quad (11)$$

In other words, the solution u of eq. (8) is a fixed point for the operator Φ^ξ , i.e. it satisfies the identity $u = \Phi^\xi(u)$.

In the next section we introduce our Neural SPDE model.

4. Neural SPDEs

Let $m, n \in \mathbb{N}$. Let $D = \{x_1, \dots, x_m\} \subset \mathcal{D}$ be a m -points discretization of the spatial domain \mathcal{D} , and let $\mathcal{T} = \{t_0, \dots, t_n\} \subset [0, T]$ be a $(n+1)$ -points discretization of the time interval $[0, T]$ with $t_0 < \dots < t_n$. Suppose the initial condition $u_0 \in \mathcal{H}_u$ is observed on D and the forcing term $\xi : [0, T] \rightarrow \mathcal{H}_\xi$ is observed on D at each time $t_i \in \mathcal{T}$.

In practice, each realization driving noise ξ is replaced by a regularized version $\delta^\epsilon * \xi$ with a compactly supported smooth mollifier δ^ϵ scaled by ϵ in space and ϵ^2 in time. From now on we take $\mathcal{H}_u = L^2(\mathcal{D}, \mathbb{C}^{d_u})$ and $\mathcal{H}_\xi = L^2(\mathcal{D}, \mathbb{C}^{d_\xi})$.

Next, we construct the Neural SPDE model according to the following three steps:

1. we first model the action of the semigroup S ,
2. then we model the action of the functions F and G ,
3. and finally we solve a neural fixed point problem.

4.1. Modelling the action of the semigroup S

For a large class of SPDEs, the action of the semigroup S can be written as an integral against a kernel function

$\mathcal{K}_t : \mathcal{D} \times \mathcal{D} \rightarrow \mathbb{C}^{d_u \times d_u}$ such that for any $h \in \mathcal{H}_u$

$$(S_t h)(x) = \int_{\mathcal{D}} \mathcal{K}_t(x, y) h(y) \mu_t(dy) \quad (12)$$

where μ_t is a Borel measure on \mathcal{D} . Here, we take μ_t to be the Lebesgue measure on \mathbb{R}^d but other choices can be made, for example to speed up computations or facilitate the learning process by incorporating prior information (Kovachki et al., 2021).

Several ways to parameterize the kernel functions \mathcal{K} have been introduced in the literature, for example using graph neural networks (Li et al., 2020b) or using the Fourier Transform (Li et al., 2020d). We follow the latter Fourier parameterization for the reasons mentioned in Sec. 2.4. For this, we assume that the kernel \mathcal{K} is stationary in space and time so that $\mathcal{K}_{t,s}(x, y) = \mathcal{K}_{t-s}(x - y)$.

Hence, as observed in Sec. 2.4, ?? can be rewritten in terms of the convolutions \star_d and \star_{d+1}

$$\Phi^\xi(u)_t = \mathcal{K}_t \star_d u_0 + (\mathcal{K} \star_{d+1} \mathbb{1}_{s \geq 0} H^{u, \xi})_t \quad (13)$$

where $\mathbb{1}_{s \geq 0}$ is the indicator function. Using the convolution theorem, eq. (13) becomes

$$\begin{aligned} \Phi^\xi(u)_t &= \mathcal{F}_d^{-1}(\mathcal{F}_d(\mathcal{K}_t) \mathcal{F}_d(u_0)) \\ &+ \mathcal{F}_{d+1}^{-1}(\mathcal{F}_{d+1}(\mathcal{K}) \mathcal{F}_{d+1}(\mathbb{1}_{s \geq 0} H^{u, \xi}))_t \end{aligned} \quad (14)$$

where all multiplications are matrix-vector multiplications.

Hence, as done for a single layer of a FNO, we parameterize the (evaluation of the) kernel \mathcal{K} directly in Fourier space as a complex tensor K_θ . Therefore, eq. (14) becomes

$$\begin{aligned} \Phi_\theta^\xi(u)_t &= \mathcal{F}_d^{-1}(\mathcal{F}_1^{-1}(K_\theta)_t \mathcal{F}_d(u_0)) \\ &+ \mathcal{F}_{d+1}^{-1}(K_\theta \mathcal{F}_{d+1}(\mathbb{1}_{s \geq 0} H_\theta^{u, \xi}))_t \end{aligned} \quad (15)$$

where we used the fact that $\mathcal{F}_d(\mathcal{K}_t) = \mathcal{F}_1^{-1}(\mathcal{F}_{d+1}(\mathcal{K}))_t$, for any $t \in [0, T]$, and used a subscript θ to denote all elements of Φ_θ^ξ parameterized by learnable parameters.

Next, we present an alternative way to model the semigroup.

4.2. Alternative way of modelling the semigroup S

The differential operators appearing in many semilinear SPDEs are of parabolic type and can be written as $\partial_t - \mathcal{L}$, where \mathcal{L} is a polynomial differential operator in space of degree m of the form

$$\mathcal{L} = \sum_{n=0}^m \sum_{\substack{k_1, \dots, k_d \\ k_1 + \dots + k_d = n}} C_{k_1, \dots, k_d} \frac{\partial^n}{\partial x_1^{k_1} \dots \partial x_d^{k_d}}, \quad (16)$$

where $C_{k_1, \dots, k_d} \in \mathbb{C}^{d_u \times d_u}$ are complex matrices.

In this case, the semigroup is an exponential $S_t = e^{t\mathcal{L}}$ and the Fourier Transform of the associated kernel \mathcal{K} is

$$\mathcal{F}_d(\mathcal{K}_t)(\omega) = e^{tP_\theta(i\omega)} \in \mathbb{C}^{d_u \times d_u} \quad (17)$$

for any $\omega \in \mathcal{D}$, where e is the matrix exponential and P_θ is the polynomial defined for any $z \in \mathbb{C}^d$

$$P_\theta(z) = \sum_{n=0}^m \sum_{\substack{k_1, \dots, k_d \\ k_1 + \dots + k_d = n}} C_{k_1, \dots, k_d} (2\pi)^n z_1^{k_1} \dots z_d^{k_d} \quad (18)$$

where the C_{k_1, \dots, k_d} are the complex matrices from eq. (16).

It follows that the operator Φ_θ^ξ can be rewritten as follows

$$\begin{aligned} \Phi_\theta^\xi(u)_t &= \mathcal{F}_d^{-1}(e^{tP_\theta(i\omega)} \mathcal{F}_d(u_0)) \\ &+ \mathcal{F}_{d+1}^{-1}(\mathcal{F}_1(e^{tP_\theta(i\omega)}) \mathcal{F}_{d+1}(\mathbb{1}_{s \geq 0} H_\theta^{u, \xi}))_t. \end{aligned} \quad (19)$$

The matrix exponential $e^{tP_\theta(i\omega)}$ can be computed either directly or via a call to an ODE solver noting that

$$\Phi_\theta^\xi(u)_t = \mathcal{F}_d^{-1}(R_t^\theta) \quad (20)$$

where R^θ is the solution of the following CDE

$$\frac{dR_t^\theta}{dt}(\omega) = P_\theta(i\omega) R_t^\theta(\omega) + \mathcal{F}_d(H_\theta^{u, \xi})_t(\omega),$$

with initial condition $R_0^\theta(\omega) = \mathcal{F}_d(u_0)(\omega)$. It remains to explain how to parameterize the function $H_\theta^{u, \xi}$.

4.3. Modelling the action of the vector fields F and G

Recall that the function $H^{u, \xi}$ is defined in eq. (11) in terms of the vector fields $F : \mathcal{H}_u \rightarrow \mathcal{H}_u$ and $G : \mathcal{H}_u \rightarrow L(\mathcal{H}_\xi, \mathcal{H}_u)$, which are assumed to satisfy some minimal Lipschitz conditions. For a large class of SPDEs arising from physics, both F and G are local operators acting on u_t and on its first partial derivatives in space ∂u_t . Thanks to the properties of the Fourier Transform $\mathcal{F}_d(u_t)$, it is easy to get the first partial derivatives of u_t in space

$$\partial u_t = \mathcal{F}_d^{-1}(\alpha \omega \mathcal{F}_d(u_t)) \quad (21)$$

where $\alpha \in \mathbb{C}$ is a complex constant. Hence, we can augment u_t with ∂u_t and use the new variable $[u_t, \partial u_t]$ as input to F and G . Because F and G act locally on $[u_t, \partial u_t]$, the evaluations $F(u_t, \partial u_t)(x)$ and $G(u_t, \partial u_t)(x)$ at any point $x \in \mathcal{D}$ only depend on the evaluations $u_t(x)$ and $\partial u_t(x)$ at x , and not on their evaluations at some other point $y \in \mathcal{D}$ in the neighbourhood of x . Typical examples of F and G are polynomials in $u_t(x)$ and $\partial u_t(x)$. Hence, we can model

them as feedforward neural networks

$$F_\theta : \mathbb{C}^{d_u(d+1)} \rightarrow \mathbb{C}^{d_u}, \quad (22)$$

$$G_\theta : \mathbb{C}^{d_u(d+1)} \rightarrow \mathbb{C}^{d_u \times d_\xi}, \quad (23)$$

acting on $[u_t, \partial u_t](x) \in \mathbb{C}^{d_u(d+1)}$, which gives

$$F(u_t, \partial u_t)(x) = F_\theta([u_t, \partial u_t](x)) \quad (24)$$

$$(G(u_t, \partial u_t)\dot{\xi}_t)(x) = G_\theta([u_t, \partial u_t](x))\dot{\xi}_t(x) \quad (25)$$

In summary, we parameterize the function $H_\theta^{u,\xi}$ as

$$H_\theta^{u,\xi}(t, x) = F_\theta([u_t, \mathcal{F}_d^{-1}(\alpha\omega\mathcal{F}_d(u_t))](x)) \quad (26)$$

$$+ G_\theta([u_t, \mathcal{F}_d^{-1}(\alpha\omega\mathcal{F}_d(u_t))](x))\dot{\xi}_t(x)$$

4.4. A neural fixed point problem

Our final Neural SPDE model consists of three components: a lift $L_\theta : \mathbb{R}^{d_u} \rightarrow \mathbb{R}^{d_h}$ to a hidden space \mathbb{R}^{d_h} , an operator Φ_θ^ξ given by the construction above, and a projection $\Pi_\theta : \mathbb{R}^{d_h} \rightarrow \mathbb{R}^{d_u}$ back to the original space \mathbb{R}^{d_u} .

The operator Φ_θ^ξ is used to solve a neural fixed point problem $z = \Phi_\theta^\xi(z)$ whose solution z is a mild solution of an SPDE in hidden space, as argued in sec. 3. Algorithmically, we proceed by Picard's iteration

$$\begin{aligned} z_t^0(x) &= L_\theta(u_0(x)), \\ z_t^{i+1}(x) &= \Phi_\theta^\xi(z^i)_t(x), \\ u_t(x) &= \Pi_\theta(z_t^M(x)) \end{aligned} \quad (27)$$

for any $t \in [0, T]$, $x \in \mathcal{D}$ and $i = 0, \dots, M-1$.

To train the neural fixed point problem in eq. (27) one needs to run backpropagation through the iterations $i = 0, \dots, M-1$. As mentioned in sections 2.1 and 2.2, it is possible to train neural differential equation models using a memory-efficient backpropagation scheme solving additional differential equations for the gradients of the loss. Bai et al. (2019) showed that there is an analogous mechanism to train neural fixed point models such as ours given in eq. (27). More precisely, they showed that the gradients of the loss function with respect to the model parameters are also solutions of a fixed point problem.

In the next section we present our experimental results on various semilinear SPDEs.

5. Experiments

Here we demonstrate how our Neural SPDE model can be used in three different supervised learning settings:

1. to learn the operator $u_0 \mapsto u$, assuming the underlying

noise ξ is not observed,

2. to learn the operator $\xi \mapsto u$, assuming the underlying noise ξ is observed but the prior data u_0 is fixed across samples,
3. to learn the operator $(u_0, \xi) \mapsto u$, assuming the underlying noise ξ is observed and that the prior data u_0 changes across samples.

We run experiments on three semilinear SPDEs: the dynamic Φ_1^4 model, the stochastic wave equation and the stochastic Navier-Stokes equation in two spatial dimensions. Note that in all the experiments below we always consider that u^{in} is equal to some initial condition $u_0 \in \mathcal{H}_u$. However, one could consider the input data u^{in} to be the values of the solution u observed over some prior time interval.

5.1. Baselines

Before presenting our experiments, we provide some extra details about the considered baselines.

Neural CDE The crucial difference between our Neural SPDE model in eq. (27) and the Neural CDE model in eq. (2) is that in the former the solution u and the driving noise ξ both take their values in functional spaces $\mathcal{H}_u, \mathcal{H}_\xi$ respectively, while in the latter u and ξ are vector-valued. Nonetheless, we note that a Neural CDE can be used in the context of SPDE-learning by considering the function u discretized on a grid D as state space of the CDE dynamics, although this results in a model that is of course not resolution-invariant. We also note that what made Neural CDEs and their variants so popular for time-series classification problems is their effective backpropagation that makes use of the adjoint sensitivity method (Pontryagin, 1987), yielding a constant memory complexity with respect to the "depth". Since they model dynamical systems, one would expect them to be applicable more broadly. However, deploying these models in situations where the loss depends on the state z_t at multiple intermediate times is more challenging (in the classification task, only the final state z_T is used to make the prediction). Indeed, the reverse-mode derivative must be broken into a sequence of separate solves, one between each consecutive pair of output times and the adjoint step has to be repeated for each interval.

Neural RDE The neural RDE model uses the depth- M log-signature transform to summarise the original input stream ξ over short time intervals and replace it with a shorter but higher dimensional stream $\text{LogSig}_M(\xi)$, which is then used to drive a Neural CDE. If ξ is d_ξ -dimensional, $\text{LogSig}_M(\xi)$ is $O(d_\xi^M)$ -dimensional. In the context of SPDE-learning, the original stream is $d_\xi|D|$ -dimensional, due to the discretization in space. Since the log-signature increases exponentially the dimensionality of the input stream,

we only consider the case $M = 2$. For $|D| = 128$ and $d_\xi = 1$ we already obtain a 8385-dimensional log-signature.

FNO What distinguishes a Neural SPDE from an FNO is the difference between the Neural SPDE operator Φ_θ defined in eq. (19) and the FNO operator $N_\theta^M \circ \dots \circ N_\theta^1$ defined in eq. (7). By construction, Φ_θ operates on the pair (z, ξ) , whilst the FNO operator is built to act on z alone (or possibly on ξ alone) and so it can't be used to handle solution operators for SPDEs depending on both z and ξ . Most importantly, weights are not shared across the different layers of a FNO, whilst they are naturally shared across the Picard's iterations of the neural fixed point defining the forward pass of a Neural SPDE. In order to use FNOs in the context of SPDE-learning, we use $\tilde{D} = [0, T] \times D$ as the new input domain, as per Remark 1 in Sec. 2.3.

Neural CDE-FNO We propose an additional baseline consisting of a Neural CDE where the drift vector fields f_θ are modelled by a FNO. More precisely, we consider

$$u_t = u_0 + \int_0^t f_\theta(u_s) ds + \int_0^t g_\theta(u_s) d\xi_s \quad (28)$$

where $f_\theta : \mathcal{H}_u \rightarrow \mathcal{H}_u$ and $g_\theta : \mathcal{H}_u \rightarrow \mathcal{L}(\mathcal{H}_\xi, \mathcal{H}_u)$, and where $\mathcal{L}(\mathcal{H}_\xi, \mathcal{H}_u)$ is the set of linear maps from \mathcal{H}_ξ to \mathcal{H}_u . By the universal approximation property of FNOs (Kovachki et al., 2021, Theorem 4) we model f_θ in eq. (28) with an FNO³. We call the resulting model Neural CDE-FNO.

DeepONet The Deep Operator Network (DeepONet) (Lu et al., 2021a) is another popular class of neural network models for learning operators on function spaces. The DeepONet architecture is based on the universal approximation theorem of Chen & Chen (1995). It consists of two sub-networks referred to as the branch and the trunk networks. The trunk acts on the coordinates $(t, x) \in [0, T] \times D$, while the branch acts on the evaluation of the initial condition u_0 on a discretized grid D . Therefore, the DeepONet is not a space resolution-invariant architecture. The output of the network is expressed as $\text{DeepONet}(u_0)(t, x) = \sum_{k=1}^p b_k(u_0) \tau_k(t, x) + b_0$, where the b_k and the τ_k are the outputs of the branch and trunk network respectively. The trunk network is usually a feedforward neural network, and one can choose the architecture of the branch network depending on the structure of the input domain. We follow Lu et al. (2021a) and use feedforward neural networks for both the trunk and the branch networks. We note that extensions of DeepONet have recently been proposed in Lu et al. (2021b), and that we plan to include these enhancements in our benchmark as future work.

³The vector field g_θ is operator valued so for simplicity we will model it with a standard feedforward neural network.

For our Neural SPDE model, we model the action of the semigroup according to Sec. 4.1, and we leave the alternative model from Sec. 4.2 as future work.

5.2. Experiments on semilinear SPDEs

For every supervised learning problem we use the unnormalized pathwise L2 loss. We use the Adam optimizer to train for 500 epochs with an initial learning rate of 0.001 that is halved every 100 epochs. For all models the readin and readout maps as well as the vector fields are modelled as feedforward neural networks. The readin and readout networks have one and two layers respectively. In the Φ_1^4 example, for all models we use $d_h = 16$ hidden units. For FNO and Neural SPDE we use the 32 maximal frequency modes both in space and time. For FNO we stack four integral operator layers as in (Li et al., 2020d). For Neural SPDE we use 4 Picard's iterations. For the Navier-Stokes example, we use the maximal 16 frequencies in space, the maximal 10 frequencies in time and $d_h = 8$.

We note that in all the equations we consider in this section, the vector fields are only locally Lipschitz. However, it can be shown (using equation-specific techniques), that a solution exists everywhere.

5.2.1. DYNAMIC Φ_1^4 MODEL

We start with the dynamic Φ^4 model in 1D, given by

$$\begin{aligned} \partial_t u - \Delta u &= 3u - u^3 + \dot{\xi}, & (t, x) &\in [0, T] \times \mathbb{T} \\ u(0, x) &= u_0(x) \end{aligned} \quad (29)$$

where \mathbb{T} denotes the 1-dimensional torus, i.e. $[0, 1]$ with endpoints identified ($\mathbb{T} = \mathbb{R}/\mathbb{Z}$). Here ξ is a space-time white noise. To generate the training dataset, we use the approximation given in Lord et al. (2014, Example 10.31) to sample realizations from the process ξ . We then solve the SPDE for each sample path using a finite difference method with 128 evenly distanced points in space and a time step size $\Delta t = 10^{-3}$. We solve the SPDE until $T = 0.05$ resulting in 50 time points. The initial condition is given by $u_0(x) = x(1 - x) + \kappa \eta(x)$, where

$$\eta(x) = \sum_{k=-10}^{k=10} \frac{a_k}{1 + |k|^2} \sin(\lambda^{-1} k \pi (x - 0.5)),$$

with $a_k \sim \mathcal{N}(0, 1)$

similar to Chevyrev et al. (2021, Equation (3.6)) with $\lambda = 2$. We either take $\kappa = 0$ or $\kappa = 0.1$ to generate a dataset where the initial data is either fixed or varies across samples.

We report the results in Table 1. The Neural SPDE model (NSPDE) obtains the lowest relative error for all tasks, and obtains nearly one order of magnitude lower relative error compared to Neural CDE models (NCDE). We note

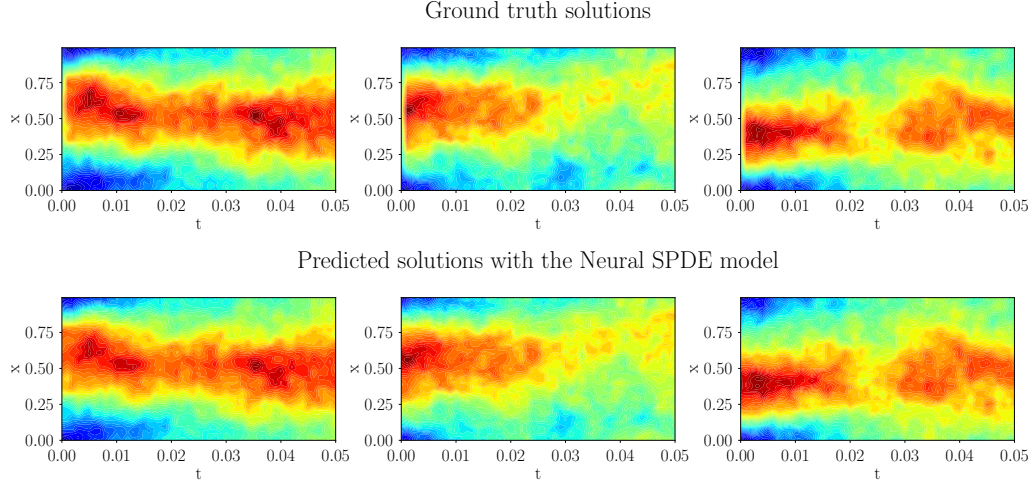


Figure 1. Ground truth and predictions on three test instances for the Φ_1^4 example.

that the Neural SPDE is the only model that can be applied to the three considered supervised learning settings.

5.2.2. STOCHASTIC WAVE EQUATION

Next we consider the wave equation with multiplicative stochastic forcing,

$$\begin{aligned} \partial_t^2 u - \Delta u &= \cos(\pi u) + u^2 + u\dot{\xi}, \quad (t, x) \in [0, T] \times \mathbb{T} \\ u(0, x) &= u_0(x) \\ \partial_t u(0, x) &= x(1 - x). \end{aligned} \quad (30)$$

We note that this SPDE is hyperbolic, and not parabolic, however the semigroup theory of Sec. 3 still applies. To generate training datasets, we solve the SPDE using a finite difference method with 128 evenly distanced points in space and a time step size $\Delta t = 10^{-3}$. We solve the SPDE until $T = 0.5$. We then downsample the temporal resolution by a factor 5, resulting in 100 time points. Here, the initial condition is given by $u_0(x) = \sin(2\pi x) + \kappa\eta(x)$, where η is defined in Equation (30). Similarly to Sec. 5.2.1 we either take $\kappa = 0$ or $\kappa = 1$ to generate datasets where the initial condition is either fixed or varies across samples. Each dataset consists of $N = 1000$ training examples.

5.2.3. STOCHASTIC NAVIER-STOKES IN 2D

We consider the vorticity equation for an incompressible two-dimensional flow,

$$\begin{aligned} \partial_t w - \nu \Delta w &= -u \cdot \nabla w + f + \sigma \dot{\xi}, \quad (t, x) \in [0, T] \times \mathbb{T}^2 \\ w(0, x) &= w_0(x), \end{aligned} \quad (31)$$

where u is the unique divergence free velocity field such that $w = \nabla \times u$ and where \mathbb{T}^2 denotes the 2-dimensional torus, i.e. $[0, 1]^2$ with opposite sides identified ($\mathbb{T}^2 = \mathbb{R}^2/\mathbb{Z}^2$). The

system is subject to both deterministic and random forces. The deterministic force f is a function of space only and is defined as in (Li et al., 2020d). The additive stochastic forcing term ξ depends on both time and space and is a Q-Wiener process which is colored in space and rescaled by $\sigma = 0.05$. We take the Q-Wiener process defined in Lord et al. (2014, Example 10.12) with $\alpha = 0.005$. The initial condition w_0 is generated according to $w_0 \sim \mathcal{N}(0, 3^{3/2}(-\Delta + 49I)^{-3})$ with periodic boundary conditions. The viscosity parameter is set to $\nu = 10^{-4}$.

We use Lord et al. (2014, Algorithm 10.6) to approximate sample paths from the Q-Wiener process. For each sample path we solve (31) with a pseudo-spectral solver (adapted from (Li et al., 2020d)) where time is advanced with a Crank–Nicolson update. We solve the SPDE on a 64×64 mesh in space and use a time step of size 10^{-3} for the Crank–Nicolson scheme. To generate training datasets for the tasks where we learn the maps $u_0 \mapsto u$ and $\xi \mapsto u$, we solve the SPDE from $t = 0$ to $t = 1$ and downsample the trajectories by a factor 10 in time (resulting in 100 time steps) and 4 in space (resulting in a 16×16 spatial resolution). The number of training samples is $N = 1000$. To generate the training dataset for the last task (where we learn the map $(u_0, \xi) \mapsto u$) we generate 10 long trajectories of 15 000 steps each from $t = 0$ to $t = 15$. We partition each of these 10 trajectories into consecutive sub-trajectories of 500 time-steps using a rolling window. This procedure yields a total of 2 000 input-output pairs. We chose to split the data into shorter sequences of 500 time steps so that one batch training could fit in memory on a Tesla P100 NVIDIA GPU. However, the model shows good performance (see Figure 2) even when evaluated on a 5 000 time step period. To showcase zero-shot super-resolution, we train the Neural SPDE model on a downsampled version of the data with 16×16

Table 1. Dynamic Φ_1^4 model. We report the relative L2 error on the test set and the runtime per batch. The symbol x indicates that the model is not applicable. In the first task ($u_0 \mapsto u$) only partial information (u_0) is provided as input; the underlying noise ξ is used to generate the dynamics, it varies across samples, but is not provided as an input to the models. This explains why the performance of the applicable models (DeepONet, FNO and NSPDE) is poorer than for all other settings. In the second setting, ($\xi \mapsto u$) the initial condition u_0 is kept fixed. In the third setting, the initial condition u_0 and the noise ξ change and are both provided as input. In these last two settings, even with a limited amount of training samples ($N = 1\,000$), the NSPDE model is able to achieve $\sim 1\%$ error rate, and marginally improves to $< 1\%$ error when $N = 10\,000$. This indicates that our model is able to capture complex dynamics even in a small data regime.

Model	$N = 1\,000$			$N = 10\,000$			Time (s)
	$u_0 \mapsto u$	$\xi \mapsto u$	$(u_0, \xi) \mapsto u$	$u_0 \mapsto u$	$\xi \mapsto u$	$(u_0, \xi) \mapsto u$	
NCDE	x	0.112	0.127	x	0.056	0.072	0.099 ± 0.005
NRDE	x	0.129	0.150	x	0.070	0.083	0.117 ± 0.005
NCDE-FNO	x	0.071	0.066	x	0.066	0.069	0.162 ± 0.009
DeepONet	0.130	0.126	x	0.126	0.061	x	0.002 ± 0.0002
FNO	0.128	0.032	x	0.126	0.027	x	0.034 ± 0.002
NSPDE (Ours)	0.128	0.009	0.012	0.126	0.006	0.006	0.026 ± 0.001

Table 2. Stochastic Wave equation. We report the relative L2 error on the test set and the runtime per batch. The symbol x indicates that the model is not applicable.

Model	$u_0 \mapsto u$	$\xi \mapsto u$	$(u_0, \xi) \mapsto u$
NCDE	x	0.142	0.432
NRDE	x	0.146	0.445
NCDE-FNO	x	0.029	0.037
DeepONet	0.190	0.143	x
FNO	0.151	0.026	x
NSPDE (Ours)	0.150	0.023	0.026

spatial resolution. After training on this coarser resolution we evaluate the model on the original resolution as shown in Figure 2. We can see that even if trained on a lower resolution the model is capable of learning the stochastic Navier-Stokes dynamics on a finer resolution.

Table 3. Stochastic Navier-Stokes equations in two dimensions. We report the relative L2 error on the test set and the runtime per batch. The symbol x indicates that the model is not applicable.

Model	$u_0 \mapsto u$	$\xi \mapsto u$	$(u_0, \xi) \mapsto u$
NCDE	x	0.366	0.843
NCDE-FNO	x	0.326	0.178
FNO	0.188	0.039	x
NSPDE (Ours)	0.155	0.034	0.049

Table 4. Ratio of the inference time of NSPDE (once trained) over the runtime of the numerical solver for different SPDEs. In each case we consider a single solution. We use the same space and time discretization for both NSPDE and the numerical solver. For the Φ_1^4 model and the stochastic wave equation we use a grid with 1 000 time points in $[0, 1]$ and 128 space points in $[0, 1]$. For the stochastic Navier-Stokes equation we use 1 000 time points in $[0, 1]$ and 64×64 space points in $[0, 1] \times [0, 1]$.

Dataset	Speedup
Dynamic Φ_1^4 model	59×
Stochastic Wave Equation	88×
Stochastic Navier-Stokes	300×

6. Conclusion and future work

By formulating the search for a mild solution of an SPDE as a neural fixed-point problem, we introduced Neural SPDEs. The Neural SPDE model extends Neural CDEs, SDEs, RDEs to operate on infinite dimensional state spaces, as well as the class of Neural Operators models to learn solution operators $(u_0, \xi) \mapsto u$ of SPDEs depending simultaneously on the initial condition u_0 and a realization of the driving noise ξ . A Neural SPDE is resolution-invariant and up to 3 orders of magnitude faster than traditional solvers. We run experiments on various semilinear SPDEs, including the 2D stochastic Navier-Stokes equations, demonstrating how Neural SPDEs are capable of learning spatiotemporal dynamics with better accuracy and using only a modest amount of training data compared to all alternative models.

We emphasise that the Neural SPDE model proposed in this paper extends, in principle, beyond the scope of SPDEs and could be used for example in computer vision applications,

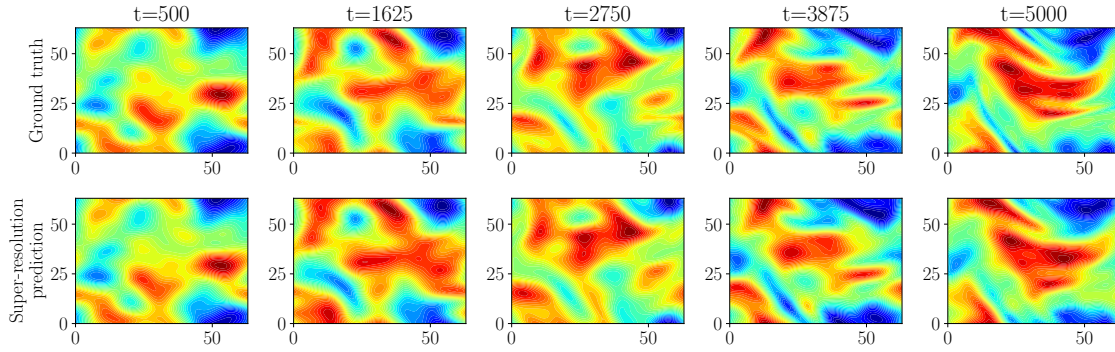


Figure 2. **Top panel:** Solution of the vorticity equation for one realisation of the stochastic forcing between the 500th and the 5000th time steps. **Bottom panel:** Predictions with the Neural SPDE model given the initial condition at the 500th time step and the forcing between the 500th and the 5000th time steps. The model is trained on a with a 16×16 mesh and evaluated on a 64×64 mesh.

which we leave as future work. We also leave as future work experimenting with the alternative way of modelling the semigroup mentioned in sec. 4.2 and the augmentation of the input variable u_t to the vector fields F and G with the first spatial derivatives ∂u_t discussed in sec. 4.3.

Acknowledgments

This project is supported by G-Research and by DataSig under the grant EP/S026347/1.

References

- Bai, S., Kolter, J. Z., and Koltun, V. Deep equilibrium models. *Advances in Neural Information Processing Systems*, 32:690–701, 2019.
- Chen, R. T., Rubanova, Y., Bettencourt, J., and Duvenaud, D. Neural ordinary differential equations. In *Proceedings of the 32nd International Conference on Neural Information Processing Systems*, pp. 6572–6583, 2018.
- Chen, T. and Chen, H. Universal approximation to nonlinear operators by neural networks with arbitrary activation functions and its application to dynamical systems. *IEEE Transactions on Neural Networks*, 6(4):911–917, 1995.
- Chevyrev, I., Gerasimovics, A., and Weber, H. Feature engineering with regularity structures. *arXiv preprint arXiv:2108.05879*, 2021.
- Ciccone, M., Gallieri, M., Masci, J., Osendorfer, C., and Gomez, F. Nais-net: Stable deep networks from non-autonomous differential equations. *arXiv preprint arXiv:1804.07209*, 2018.
- Hairer, M. An introduction to stochastic pdes. *arXiv preprint arXiv:0907.4178*, 2009.
- Hairer, M. Solving the kpz equation. *Annals of mathematics*, pp. 559–664, 2013.
- Hairer, M. A theory of regularity structures. *Inventiones mathematicae*, 198(2):269–504, 2014.
- Holden, H., Øksendal, B., Ubøe, J., and Zhang, T. Stochastic partial differential equations. In *Stochastic partial differential equations*, pp. 141–191. Springer, 1996.
- Kidger, P., Morrill, J., Foster, J., and Lyons, T. Neural controlled differential equations for irregular time series. *arXiv preprint arXiv:2005.08926*, 2020.
- Kidger, P., Foster, J., Li, X., Oberhauser, H., and Lyons, T. Neural sdes as infinite-dimensional gans. *arXiv preprint arXiv:2102.03657*, 2021.
- Kleinert, H. and Schulte-Frohlinde, V. *Critical properties of phi4-theories*. World Scientific, 2001.
- Kovachki, N., Li, Z., Liu, B., Azizzadenesheli, K., Bhattacharya, K., Stuart, A., and Anandkumar, A. Neural operator: Learning maps between function spaces. *arXiv preprint arXiv:2108.08481*, 2021.
- Li, X., Wong, T.-K. L., Chen, R. T., and Duvenaud, D. Scalable gradients for stochastic differential equations. In *International Conference on Artificial Intelligence and Statistics*, pp. 3870–3882. PMLR, 2020a.
- Li, Z., Kovachki, N., Azizzadenesheli, K., Liu, B., Bhattacharya, K., Stuart, A., and Anandkumar, A. Neural operator: Graph kernel network for partial differential equations. *arXiv preprint arXiv:2003.03485*, 2020b.
- Li, Z., Kovachki, N., Azizzadenesheli, K., Liu, B., Stuart, A., Bhattacharya, K., and Anandkumar, A. Multipole graph neural operator for parametric partial differential equations. *Advances in Neural Information Processing Systems*, 33, 2020c.
- Li, Z., Kovachki, N. B., Azizzadenesheli, K., Bhattacharya, K., Stuart, A., Anandkumar, A., et al. Fourier neural operator for parametric partial differential equations. In

- International Conference on Learning Representations*, 2020d.
- Lord, G. J., Powell, C. E., and Shardlow, T. *An introduction to computational stochastic PDEs*, volume 50. Cambridge University Press, 2014.
- Lu, L., Jin, P., Pang, G., Zhang, Z., and Karniadakis, G. E. Learning nonlinear operators via deeponet based on the universal approximation theorem of operators. *Nature Machine Intelligence*, 3(3):218–229, 2021a.
- Lu, L., Meng, X., Cai, S., Mao, Z., Goswami, S., Zhang, Z., and Karniadakis, G. E. A comprehensive and fair comparison of two neural operators (with practical extensions) based on fair data. *arXiv preprint arXiv:2111.05512*, 2021b.
- Lyons, T. Rough paths, signatures and the modelling of functions on streams. *arXiv preprint arXiv:1405.4537*, 2014.
- Lyons, T. J. Differential equations driven by rough signals. *Revista Matemática Iberoamericana*, 14(2):215–310, 1998.
- Lyons, T. J., Caruana, M., and Lévy, T. *Differential equations driven by rough paths*. Springer, 2007.
- Mikulevicius, R. and Rozovskii, B. L. Stochastic navier–stokes equations for turbulent flows. *SIAM Journal on Mathematical Analysis*, 35(5):1250–1310, 2004.
- Morrill, J., Salvi, C., Kidger, P., and Foster, J. Neural rough differential equations for long time series. In *International Conference on Machine Learning*, pp. 7829–7838. PMLR, 2021.
- Pontryagin, L. S. *Mathematical theory of optimal processes*. CRC press, 1987.